LMI-based Robust Control for Flexible Spacecraft Systems with Input Magnitude and Rate Saturations

Lu Wang, Jiaqi Zhong, Xi Yuan, Zeyu Zheng, Dengpan Wang, Fei Wang, Hao Wang, Dou Zhang

***Abstract*—Few studies have addressed the robustness of flexible spacecraft (FS) systems in the presence of input magnitudes and rate saturations. Thus, the present work is conducted to provide more information in this field and to propose a linear matrix inequality (LMI)-based H_∞ controller for a class of flexible spacecraft systems described by the two nonlinear dynamic models. First, a standard state-space representation is obtained by analyzing the characteristics of the rotation angle. Then, based on the assumption that the input constraints are negligible, a sufficient condition is derived by applying the definition of the H_∞ controller and exponential stability. In addition, a constrained controller is developed to ensure the saturation of the input magnitude and rate using an invariant set. Finally, two simulations with various conditions are carried out to evaluate the performance of the proposed methodology.**

***Index Terms*—flexible spacecraft system, input magnitude saturation, rate saturation, H_∞ control, LMI**

I. Introduction

THERE are many flexible structures that have attracted widely attention recently for their light weight, high efficiency, low energy requirement, and cost-effectiveness compared with the traditional structures [1] . In aerospace engineering applications, flexible structures have been used in spacecraft systems [2]–[3] , that involve a central rigid body. To absorb more energy from solar radiation, the attitude of the flexible appendages must be changed according to the angle of intersection between the spacecraft and the sun. However, due to the flexibility of structure, the external disturbances cause the irregular propagation of elastic oscillations. Moreover, the constraints of controller also impact the dynamic property and even cause system instability. Hence, a constrained controller should be designed for flexible spacecraft systems to ensure robustness and solve the high-precision attitude problem.

Researchers have proposed many control strategies for different models of FS. Hu [4] proposed a sliding mode–based discontinuous controller to address the vibration problem. To solve the problem of actuator nonlinearity and uncertainties, a fault-tolerant tracking method was proposed in Ref. [5], which combined Neural networks and sliding-mode controller. Zhong et al. [6] proposed a disturbance compensator-based controller using the internal model principle to ensure system robustness. Dong et al. [7] proposed a high-precision attitude controller combining a nonlinear predictor and a sliding-mode method to enhance stabilization of a networked FS system with uncertainties and induced delays. For the controller design of flexible structures, it is a key problem that can decrease the disturbances associated with the dynamic characteristics between the different components.

Actuator saturation is a typical problem in practical control systems. The inherent nonlinear characteristics of flexible spacecraft can have a significant impact on different control systems. Many methods can be used to treat the stabilization problem of constrained systems, such as invariant set approach [8], anti-windup method [9], barrier Lyapunov functions approach [10], and predictive control method [11]. The state of a system approaches zero according to the definition of the stabilization, implying a relationship between the Lyapunov function and the actuator saturation [12]. The design of an appropriate invariant set for different controller formulations is difficult. The anti-windup method [13] is usually used for a constrained system to decrease the impact of saturation and improve system stability. But the system with an anti-windup compensator increases the complexity, which reduces the ability to implement it in practical engineering. Each initial condition for a class of nonlinear systems yields different sets on the barrier Lyapunov function [14]. But choosing a relevant function is a difficult problem, especially for a complex system. The predictive controller [15] can provide the optimal input every time using the optimal online strategy and yields a high computational burden. To date, few studies have been conducted on accurate robustness performance index of constrained systems.

Manuscript received May 19, 2022; revised December 21, 2022.

This work was supported by the Development Fund Project of China Electronic Technology Group Corporation (NO. K01103JT202101), and the State Key Laboratory of Powder Metallurgy, Central South University.

L. Wang is a PhD candidate of State Key Laboratory of Powder Metallurgy, Central South University, Changsha, Hunan, 410083, China. (e-mail: wanglu720@163.com).

J. Zhong is an assistant professor of Chongqing University of Posts and Telecommunications, Chongqing 400065, China (e-mail: zhongjq@cqupt.edu.cn).

X. Yuan is an assistant professor of College of Chemistry and Chemical Engineering, Central South University, Changsha, Hunan, 410083, China (e-mail: xiyuan@csu.edu.cn).

Z. Zheng is a senior engineer of CETC Chips Technology Group CO., LTD, Chongqing 401332, China (e-mail: 13752882051@163.com).

D. Wang is a senior engineer of CETC Chips Technology Group CO., LTD, Chongqing 401332, China (e-mail: wangdengpan168@163.com).

F. Wang is an engineer of CETC Chips Technology Group CO., LTD, Chongqing 401332, China (e-mail: wangf524@163.com).

H. Wang is a senior engineer of CETC Chips Technology Group CO., LTD, Chongqing 401332, China (e-mail: 158736214@qq.com).

D. Zhang is a professor of State Key Laboratory of Powder Metallurgy, Central South University, Changsha, Hunan, 410083, China. (Phone: 86-13875862109; fax: 86-0731-88877196; e-mail: dzhang@csu.edu.cn).

Furthermore, the rate saturation is an important constraint for the safe operation of flexible spacecraft systems [16]–[17]. Zou et al. [18] proposed a tracking controller to stabilize the augmented model using a smooth tangent function by combining the back stepping, robust and adaptive methods. To estimate external disturbance, Liu et al. [19] proposed a disturbance observer to stabilize the original nonlinear model using a framework of linear matrix inequality (LMI). Moreover, an integral state controller with a linear quadratic regulator was proposed by Moghimi Rad et al. [20] to overcome the problem of actuator constraints for an autonomous aerial vehicle by employing an anti-windup compensator. Currently, there is no common method to treat the rate saturation problem, which is difficult for the controller designing of a flexible spacecraft system.

To address the problem of such system with bounded external disturbances, input magnitude saturation and rate saturation, a constrained controller is proposed in this study using the H_∞ norm, exponential stability theory, invariant set approach, and the LMI. Compared with previous studies, potential contributions can be summarized as follows:

- Unlike other H_∞ controllers for a flexible spacecraft [21]–[22], an original model with input magnitude and rate saturations has been considered. The proposed controller, based on the linearized state-space representation, can deal with more general actuator constraints by applying the Lyapunov method, invariant set theory and H_∞ norm.
- In contrast to other anti-interference control methods [2],[19] an LMI-based optimization problem is analytically proposed to obtain an optimal control gain that can improve the performance of interference suppression under the given constraints.

The subsequent content of the manuscript is organized as follows. First, the nonlinear model of a FS system is designed and transformed into a standard state-space representation. Second, a sufficient parameter of the H_∞ controller is presented and placed within the LMI constraints. Third, two numerical simulations for different conditions are provided to demonstrate the proposed methodology's property. Finally, the conclusions are proposed.

Notation: $\Re^n$ denotes the set of Euclidean space; I stands for the identity matrix; T refer to the transpose operation; the symbol * means the ellipsis in matrix.

II. Model Description

This study focuses on a class of FS that rotates around a single axis. The FS has a rigid body and uniform flexible appendages (Fig. 1).

To describe the dynamical characteristics, we can place the flexible spacecraft on the different coordinate system. Hence, we can describe the model of FS [19] as follows:

$$J\ddot{\theta}(t)+F^T\ddot{q}(t)=u(t)+d_0(t) \tag{1}$$

$$\ddot{q}(t)+T\dot{q}(t)+Sq(t)+F\ddot{\theta}(t)=0 \tag{2}$$

where $\theta(t)\in\Re^n$ is the rotation angle of the body-fixed frame on the coordinate system; $J\in\Re^n$ refers to inertia moment; $d_0(t)\in\Re^n$ means the bounded external disturbance torques, such as space environmental torques; $q(t)\in\Re^n$ means the modal coordinate vector ; $F\in\Re^n$ represents the coupling matrix between different dynamics; $T=diag\{2\xi_1\omega_1,\cdots 2\xi_n\omega_n\}\in\Re^{n\times n}$ and $S=diag\{\omega_1^2,\cdots\omega_n^2\}$ refer to the damping and stiffness matrices; ω_n refers to natural frequency, ξ_n means damping ratio; $u(t)\in\Re^n$ denotes the control torque.

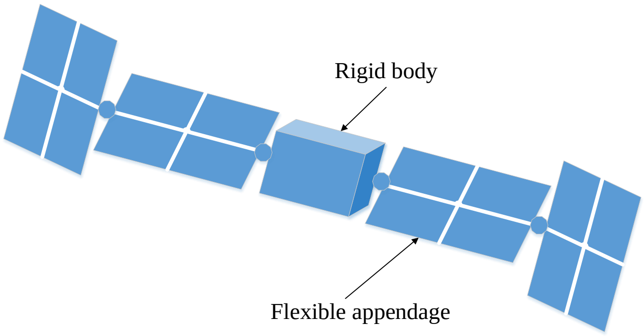

Fig. 1. Diagram of a FS system

Evidently, the dynamic characteristics of the FS can be described by models (1) and (2), which are high-dimensional. The high-dimensional characteristics can be ignored to simplify the controller design. Hence, applying the modal truncation method can give the low-dimensional model, capturing the dominant characteristics for vibration suppression. Only the first two modes are considered in this study with stable generality. By denoting $x(t)=\begin{bmatrix}\theta(t) & \dot{\theta}(t)\end{bmatrix}^T$, we can express the nonlinear models (1) and (2) as follows:

$$\dot{x}(t)=Ax(t)+Bu(t)+B\omega(t) \tag{3}$$

where $A=\begin{bmatrix}0 & I\\ 0 & 0\end{bmatrix}$, $B=\begin{bmatrix}0\\ \left(J-FF^T\right)^{-1}\end{bmatrix}$ and $\omega(t)=d_0(t)+F\left(T\dot{q}(t)+Cq(t)\right)$. To describe the global performance, the output equation can be defined as

$$y(t)=Cx(t) \tag{4}$$

where C is the output vector.

The objective is to design an H_∞ controller, subject to the bounded external disturbance $\omega_{\max}=\int_0^t\|\omega(t)\|_2^2\,dt$, input magnitude $|u(t)|\le u_{\max}$ and rate constraint $|\dot{u}(t)|\le v_{\max}$. For the whole initial conditions, the stabilization and robustness of such system can be satisfied.

III. Constrained H_∞ Controller Design

To reach the aforementioned aim, this paper used the H_∞ norm to suppress external disturbances. Subsequently, a constrained controller is proposed under condition of the relevant constraints. Defining the control gain K, the input can be expressed as

$$u(t) = Kx(t) \quad (5)$$

Substituting formula (5) into (3), the closed-loop state equation of the FS without the above two constraints can be transformed as follows:

$$\dot{x}(t) = Ax(t) + BKx(t) + B\omega(t) \quad (6)$$

Hence, the following theorems can be obtained:

Theorem 1: Considering the closed-loop systems described by formula (4) and (6), if there exists a parameter $\gamma > 0$ and matrices $X > 0$, with Y satisfying

$$\begin{bmatrix} AX + BY + * + 2\rho X & XC^T & B \\ * & -I & 0 \\ * & * & -\gamma^2 I \end{bmatrix} < 0 \quad (7)$$

then the closed-loop system of flexible spacecraft is exponentially stable with the decay rate ρ and H_∞ gain from $\omega(t)$ to $y(t)$ is γ. In this case, the control gain matrix K is given by

$$K = YX^{-1} \quad (8)$$

Proof. We first consider the following function

$$V(t) = x^T(t) P x(t) \quad (9)$$

Considering the time derivative of $V(t)$ along the trajectory of the system, we obtain

$$\begin{aligned} \dot{V}(t) &= \dot{x}^T(t) P x(t) + x^T(t) P \dot{x}(t) \\ &= \left(Ax(t) + BKx(t) + B\omega(t)\right)^T Px(t) \\ &\quad + x^T(t) P\left(Ax(t) + BKx(t) + B\omega(t)\right) \\ &= \begin{bmatrix} x^T(t) & \omega^T(t) \end{bmatrix} \begin{bmatrix} PA + PBK + * & PB \\ * & 0 \end{bmatrix} \begin{bmatrix} x(t) \\ \omega(t) \end{bmatrix} \end{aligned} \quad (10)$$

Subsequently, we introduce the exponential stability as follows:

$$\dot{V}(t) + 2\rho V(t) < 0 \quad (11)$$

Multiplying (11) by $e^{2\rho t}$ yields

$$e^{2\rho t}\dot{V}(t) + 2\rho e^{2\rho t} V(t) = \frac{d\left(e^{2\rho t} V(t)\right)}{dt} < 0 \quad (12)$$

By integrating (12) in $[0 \quad t]$, the following equation can be obtained

$$\begin{aligned} \int_0^t \frac{d\left(e^{2\rho t} V(t)\right)}{dt} dt &= e^{2\rho t} V(t) - V(0) \\ &= e^{2\rho t} x^T(t) P x(t) - x^T(0) P x(0) < 0 \end{aligned} \quad (13)$$

Herein, the relationship between $x(t)$ and $x(0)$ can be described as follows:

$$|x(t)|^2 < e^{-2\rho t} |x(0)|^2 \quad (14)$$

Evidently, $x(t)$ converges to zero with ρ and the sufficient condition on matrix inequality can be expressed as

$$\dot{V}(t) + \rho V(t) = \begin{bmatrix} PA + PBK + * + 2\rho P & PB \\ * & 0 \end{bmatrix} < 0 \quad (15)$$

From the view of the mathematics, it is impossible to obtain a feasible solution because there is zero in the principal minor. Thus, the definition of H_∞ norm is introduced as follows:

$$\dot{V}(t) + 2\rho V(t) + y^T(t) y(t) - \gamma^2 \omega^T(t) \omega(t) < 0 \quad (16)$$

Substituting (4) and (15) into (16), the inequality holds:

$$\begin{bmatrix} PA + PBK + * + 2\rho P + C^T C & PB \\ * & -\gamma^2 I \end{bmatrix} < 0 \quad (17)$$

Applying the Schur Complement lemma, (17) is transformed as

$$\begin{bmatrix} PA + PBK + * + 2\rho P & C^T & PB \\ * & -I & 0 \\ * & * & -\gamma^2 I \end{bmatrix} < 0 \quad (18)$$

However, the above bilinear matrix inequality cannot be solved due to its non-convex characteristics. Pre- and post-multiplying (18) with matrix $diag\{P^{-1} \quad I \quad I\}$ yields

$$\begin{bmatrix} AP^{-1} + BKP^{-1} + * + 2\rho P^{-1} & P^{-1}C^T & B \\ * & -I & 0 \\ * & * & -\gamma^2 I \end{bmatrix} < 0 \quad (19)$$

By defining $X = P^{-1}$ and $Y = KP^{-1}$, (7) can be obtained.

The aforementioned analysis proposes a sufficient condition (7) on the H_∞ norm of such system. We usually minimize the H_∞ gain but increase the control gain K, which maximizes the input. To keep balance between the input constraints and high-property index, the theorem 2 is presented.

Theorem 2: Consider the closed-loop flexible spacecraft systems (4) and (6) with the input saturation $|u(t)| < u_{\max}$ and the rate constraint $|\dot{u}(t)| < v_{\max}$. If defined positive scalars ρ and ξ exist, as well as undefined positive scalar γ, matrix $X > 0$ and vector Y, there exists an LMI optimization question as follows:

$$\min_{\gamma>0, X>0, Y} \gamma \quad (20)$$

Subject to (7) and

$$\begin{bmatrix} X & * \\ Y & \xi^{-1} u_{\max}^2 \end{bmatrix} > 0 \quad (21)$$

$$\begin{bmatrix} v_{\max}^2 / u_{\max}^2 \cdot X & * \\ AX + BY & X \end{bmatrix} \geq 0 \quad (22)$$

$$\begin{bmatrix} v_{\max}^2 / u_{\max}^2 I & * \\ B & X \end{bmatrix} \geq 0 \quad (23)$$

$$\begin{bmatrix} \xi - \gamma^2 W_{\max} & * \\ x(0) & X \end{bmatrix} > 0 \quad (24)$$

$$\begin{bmatrix} 0.5\xi - \gamma^2 W_{\max} - W_{\max} & * \\ x(0) & X \end{bmatrix} > 0 \quad (25)$$

The H_∞ controller of FS can be expressed as

$$u(t) = YX^{-1} x(t) \quad (26)$$

which satisfies the given input saturation $u_{\max}$ and rate constraint $v_{\max}$.

Proof: First, let us analyze the relationship between $u(t)$ and $V(t)$. Applying the Schur Complement lemma, (21) transforms into $K^T K \le \xi^{-1} u_{\max}^2 P$. Thus, we have the following inequality

$$\begin{aligned} u^2(t) &= (Kx)^T Kx = x^T K^T K x \\ &\le \xi^{-1} u_{\max}^2 x^T P x = \xi^{-1} u_{\max}^2 V(t) \le u_{\max}^2 \end{aligned} \quad (27)$$

Hence, (27) means $\xi^{-1} V(t) \le 1$. By integrating (16) within $[0 \quad t]$, the association of $V(0)$ and $V(t)$ can be expressed as follows:

$$V(t) < V(0) + \gamma^2 \int_0^t \omega^T(t) \omega(t) dt = V(0) + \gamma^2 W_{\max} \quad (28)$$

where $W_{\max} = \int_0^t \omega^T(t)\omega(t) dt$. Herein, the invariant set can be rewritten as

$$\xi^{-1} x^T(0) P x(0) + \xi^{-1} \gamma^2 W_{\max} < 1 \quad (29)$$

Using the Schur Complement lemma once again, (29) is expressed as follows:

$$\begin{bmatrix} \xi - \gamma^2 W_{\max} & x(0) \\ * & P^{-1} \end{bmatrix} > 0 \quad (30)$$

By denoting $X = P^{-1}$, (24) can be obtained. Furthermore, the problem of rate constraint, that is, $|\dot{u}(t)| \le v_{\max}$, is discussed. The rate of input can be expressed as

$$\dot{u}(t) = K\dot{x}(t) = K\left(Ax(t) + BKx(t) + B\omega(t)\right) \quad (31)$$

Based on the assumption that

$$(A+BK)^T P (A+BK) \le v_{\max}^2 / u_{\max}^2 P \quad (32)$$

$$B^T P B \le v_{\max}^2 / u_{\max}^2 I \quad (33)$$

the rate constraint is rewritten as

$$\begin{aligned} \dot{u}^2(t) &= (Ax + BKx + B\omega)^T K^T K (Ax + BKx + B\omega) \\ &\le 2x^T(t)(A+BK)^T K^T K (A+BK) x(t) \\ &\quad + 2\omega^T(t) B^T K^T K B \omega(t) \\ &\le 2\xi^{-1} u_{\max}^2 x^T(t)(A+BK)^T P (A+BK) x(t) \\ &\quad + 2\xi^{-1} u_{\max}^2 \omega^T(t) B^T P B \omega(t) \\ &\le 2\xi^{-1} v_{\max}^2 x^T(t) P x(t) \\ &\quad + 2\xi^{-1} v_{\max}^2 \omega^T(t) \omega(t) \\ &= 2\xi^{-1} v_{\max}^2 \left(V(t) + \omega^T(t)\omega(t)\right) \end{aligned} \quad (34)$$

Hence, we have

$$\begin{aligned} & 2\xi^{-1} x^T(0) P x(0) + 2\xi^{-1} \gamma^2 W_{\max} + 2\xi^{-1} \omega^T(t) \omega(t) \\ & < 2\xi^{-1} x^T(0) P x(0) + 2\xi^{-1} \gamma^2 W_{\max} + 2\xi^{-1} \omega_{\max}^T \omega_{\max} \\ & < 2\xi^{-1} x^T(0) P x(0) + 2\xi^{-1} \gamma^2 W_{\max} + 2\xi^{-1} W_{\max} \\ & < 1 \end{aligned} \quad (35)$$

Moreover, (35) can be expressed as

$$x^T(0) P x(0) < 0.5\xi - \gamma^2 W_{\max} - W_{\max} \quad (36)$$

Application of Schur complement lemma to (36) gives the following matrix inequality:

$$\begin{bmatrix} 0.5\xi - \gamma^2 W_{\max} - W_{\max} & * \\ x(0) & P^{-1} \end{bmatrix} > 0 \quad (37)$$

By denoting $X = P^{-1}$, (25) can be held. Using a similar procedure, (32) and (33) can be transformed into

$$\begin{bmatrix} v_{\max}^2 / u_{\max}^2 P & * \\ A + BK & P^{-1} \end{bmatrix} \ge 0 \quad (38)$$

$$\begin{bmatrix} v_{\max}^2 / u_{\max}^2 I & * \\ B & P^{-1} \end{bmatrix} \ge 0 \quad (39)$$

Pre- and post-multiplying (38) and (39) with the block diagonal matrix $diag\{P^{-1} \quad I\}$ yields (22).

IV. Simulation

To evaluate the property of the proposed controller (5) in term of optimization problem (20), the simulation is carried out for a model of FS. For comparison, the same controller with different constraints can be substituted into the model of the FS. The moment of inertia and coupling matrix can be defined as follows [2]:

$$J = \begin{bmatrix} 350 & 3 & 4 \\ * & 280 & 10 \\ * & * & 190 \end{bmatrix} \text{kg} \cdot \text{m}^2$$

$$F = \begin{bmatrix} 6.4564 & 1.2782 & 2.1563 \\ -1.2582 & 0.9176 & -1.6726 \\ 1.1169 & 2.4890 & -0.8367 \end{bmatrix} \text{kg}^{1/2} \cdot \text{m}^2/\text{s}^2$$

TABLE I gives the first three natural frequencies of the FS.

TABLE I
Natural frequency and damping ratio of the FS

Parameter	Description	Value
ω_1	Natural frequency (NF) of the first mode	0.7681 rad/s
ω_2	NF of the second mode	1.1038 rad/s
ω_3	NF of the third mode	1.873 rad/s
ξ_1	Damping ratio (DR) of the first mode	0.0336
ξ_2	DR of the second mode	0.0516
ξ_3	DR of the third mode	0.078

Furthermore, the external disturbance $d_0(t)$ of this system is assumed to be

$$d_0(t) = \begin{cases} d_{01} = 0.002\left[\cos(0.03t) + 2\sin(0.06t) + 1\right] \text{N}\cdot\text{m} \\ d_{02} = 0.002\left[-\sin(0.03t) + 2\cos(0.06t) + 1\right] \text{N}\cdot\text{m} \\ d_{03} = 0.002\left[\cos(0.03t) - 2\cos(0.06t) - 1\right] \text{N}\cdot\text{m} \end{cases}$$

The initial rotation angle θ is defined as $\theta(0) = [\pi/6 \quad \pi/6 \quad \pi/6]^T$, and the initial angular velocity is assumed to be $\dot{\theta}(0) = [0 \quad 0 \quad 0]^T$. The initial modal coordinate vector is also defined as $q(0) = [0.1\sin(0.1t) \quad 0.1\sin(0.2t) \quad 0.2\sin(0.5t)]^T$.

The aforementioned parameters can be substituted into (1) and (2), whose dynamic characteristics can be obtained using MATLAB. Subsequently, the H_∞ control gain can be obtained using the input constraints. Based on the assumption that the input saturation $u_{\max}$ is $100\ \text{N}\cdot\text{m}$, rate saturation $v_{\max}$ is 100, decay rate ρ is 0.1, output vector C is

$\begin{bmatrix}1 & 1 & 1 & 1 & 1 & 1\end{bmatrix}$, and positive scalar ξ is 18, application of the LMI toolbox can give the numerical solution to the optimization problem (20). Thus, we can obtain $\gamma = 0.0208$, X and Y.

Using (26), the constrained H_∞ control gain can be obtained as

$$K = \begin{bmatrix} -19.1702 & -14.6240 & -13.8875 & -69.0007 & -6.5204 & -1.7820 \\ -14.8976 & -18.5508 & -14.2374 & -13.4795 & -67.1374 & -10.4546 \\ -18.5762 & -18.6693 & -21.0550 & -47.9423 & -49.2091 & -83.0097 \end{bmatrix}.$$

Thus, the dynamic characteristics of this system are obtained. The trajectories of rotation angles, angular velocity and output can reflect the proposed H_∞ controller performance (Fig. 2–Fig. 4). Due to external disturbances and due to strict constraints, it is difficult for the state variable $x(t)$ to approach zero. The control of torques and rates illustrates that the inputs can also satisfy the requirement of the constraints (Fig. 5, 6).

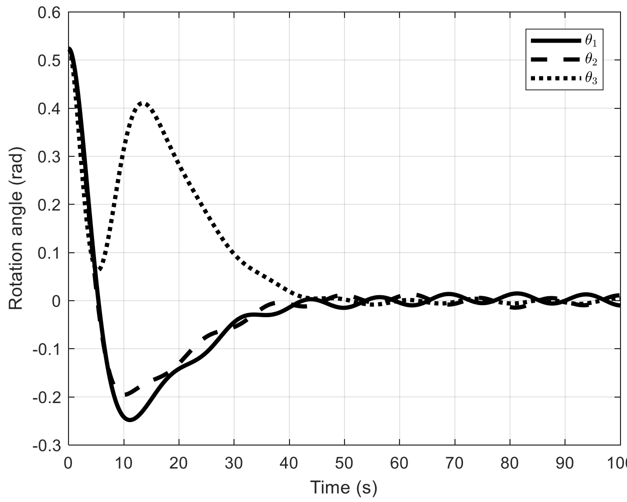

Fig. 2. Trajectories of rotation angles using the H_∞ controller at input saturation $u_{\max} = 100$ and rate saturation $v_{\max} = 100$

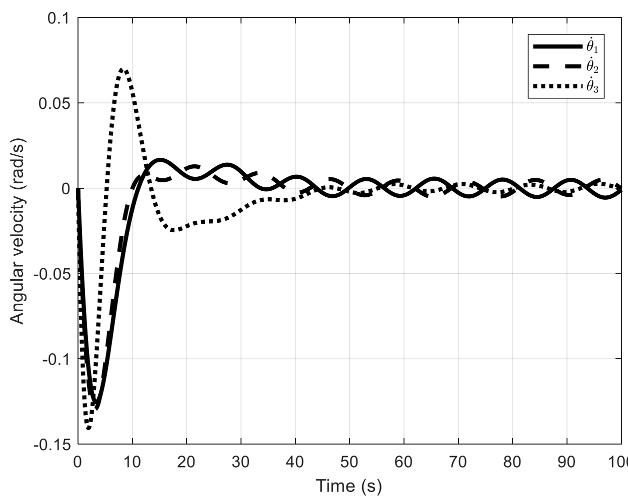

Fig. 3. Trajectories of angular velocity using the H_∞ controller at input saturation $u_{\max} = 100$ and rate saturation $v_{\max} = 100$

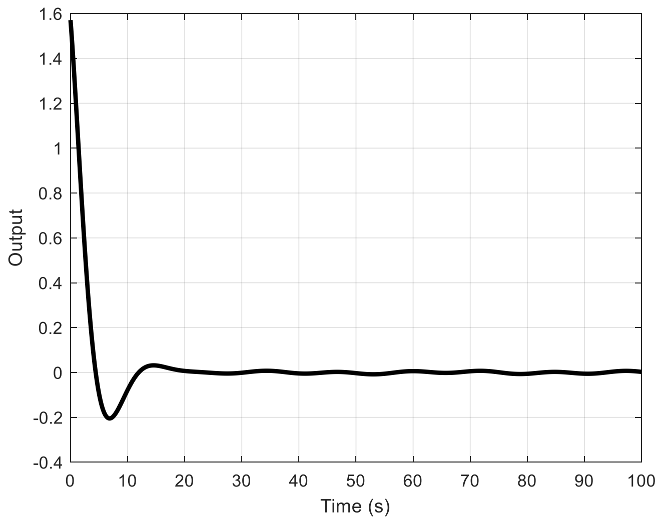

Fig. 4. Trajectory of output using the H_∞ controller at input saturation $u_{\max} = 100$ and rate saturation $v_{\max} = 100$

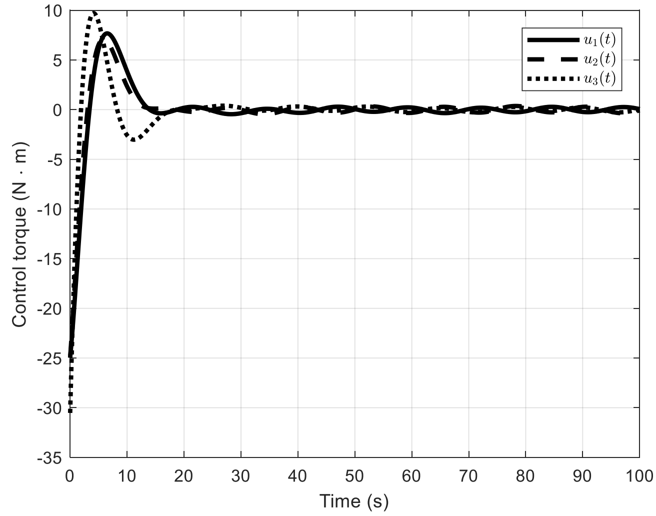

Fig. 5. Control torques of H_∞ controller at input saturation $u_{\max} = 100$ and rate saturation $v_{\max} = 100$

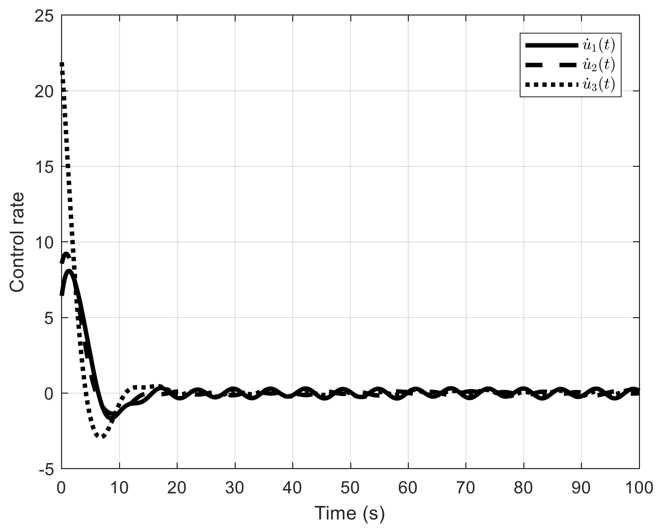

Fig. 6. Control rates of H_∞ controller at input saturation $u_{\max} = 100$ and rate saturation $v_{\max} = 100$

However, the input constraints degrade the dynamical characteristics of the system because of a balance between the high-property index and system constraints. Strictly speaking, the rotation angle and angular velocity have relatively large fluctuations, which are not suitable for the normal operation of a FS. Although the proposed methodology can enhance the stability of such system, the constraints of the actuators may produce an output that cannot satisfy the dynamic characteristics. To evaluate the effectiveness of such controller, we define $u_{\max}=500$, $v_{\max}=500$ and $\xi=3$. Application of the LMI toolbox can also give $\gamma=1.028\times10^{-4}$, X and Y .

Similarly, the new H_∞ control gain can be obtained as

$$K=\begin{bmatrix}-66.2283 & -61.8393 & -61.5609 & -162.9145 & -100.3534 & -96.4840\\ -64.4642 & -68.2859 & -64.3768 & -105.6966 & -160.2164 & -104.5284\\ -92.5959 & -92.7907 & -95.4631 & -154.4290 & -157.1433 & -195.0540\end{bmatrix}.$$

Subsequently, the rotation angles and the output of the flexible spacecraft (Fig. 7–Fig. 9) can be determined. The comparison of the dynamic characteristics of the system at different input constraints, that is, $u_{\max}=v_{\max}=100$ and $u_{\max}=v_{\max}=500$, shows that the time of the transient state decreases by a large amount. This comparison also shows that the performance of interference suppression is enhanced which is indicated by the robust performance index γ .

Furthermore, the control torques and rates are investigated under the given constraints (Fig. 10–Fig. 11). Evidently, the proposed H_∞ controller can effectively restrict the inputs. However, the input cannot approach the maximum value because the redundant control will be applied to respond to the unknown external disturbances (Fig. 5, 6, 10, 11). Therefore, the simulation results verified the performance of that controller from different perspectives of the closed-loop model.

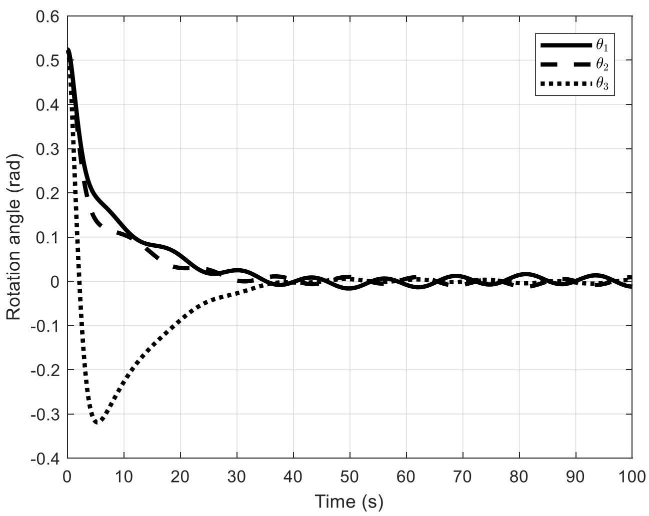

Fig. 7. Trajectories of rotation angles using H_∞ controller at input saturation $u_{\max}=500$ and rate saturation $v_{\max}=500$

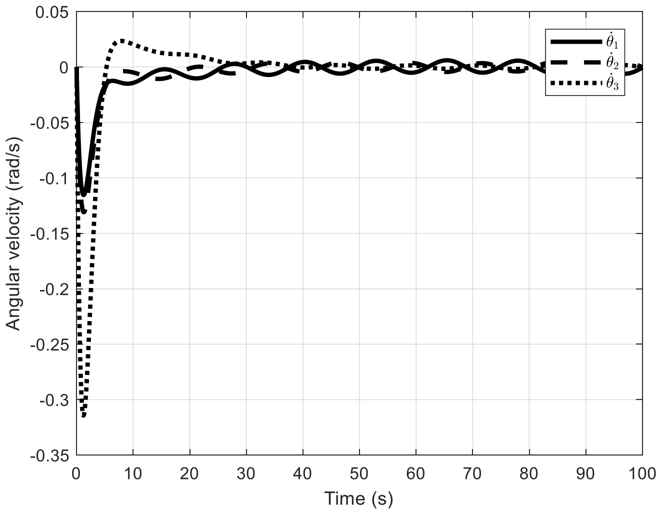

Fig. 8. Trajectories of angular velocity using H_∞ controller at input saturation $u_{\max}=500$ and rate saturation $v_{\max}=500$

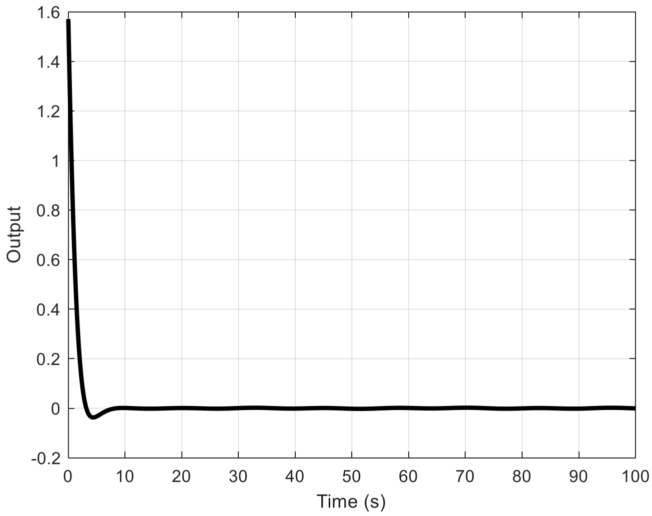

Fig. 9. Trajectory of output using H_∞ controller at input saturation $u_{\max}=500$ and rate saturation $v_{\max}=500$

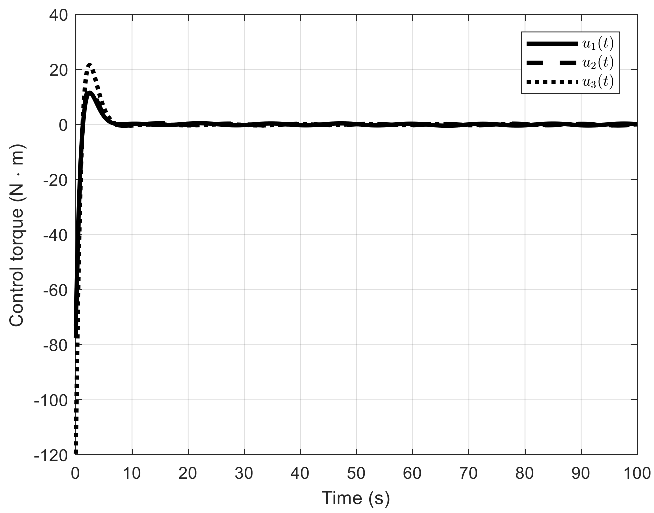

Fig. 10. Control torques of H_∞ controller at input saturation $u_{\max}=500$ and rate saturation $v_{\max}=500$

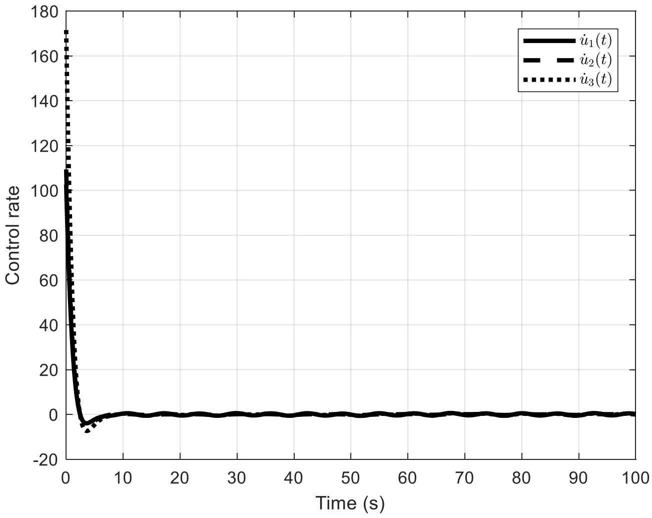

Fig. 11. Control rates of H_∞ controller at input saturation $u_{\max} = 500$ and rate saturation $v_{\max} = 500$

V. CONCLUSIONS

This study investigates the robust control problem for a typical FS system subject to bounded outer disturbance, input magnitude saturation, and rate saturation. A constrained H_∞ state feedback control is established to ensure the stabilization of a closed-loop system and suppress the outer disturbances. The nonlinear model of the FS is transformed as a typical state-space equation with nonlinear external disturbances. Based on the definition of norm and exponential stability, a sufficient condition is obtained based on LMI approach. Application of the invariant set theory can also limit the manipulated input based on input saturation and rate limitation. The control gain can be determined based on treating convex problem so as to enhance the property of the closed-loop system. The simulation results reflect that the performance of the proposed methodology can meet the requirement. Future research will extend the present results to the flexible spacecraft model described by nonlinear partial differential equations.

REFERENCES

[1] J. Zhong, X. Chen, Y. Yuan, and J. Tan, "LMI-based hybrid temporal-spatial differential control design for a class of Euler-Bernoulli beam system," Proceedings of the Institution of Mechanical Engineers, Part C: Journal of Mechanical Engineering Science, vol. 235, no.24, pp7859-7869, 2021.

[2] T. He, and Z. Wu, "Iterative learning disturbance observer based attitude stabilization of flexible spacecraft subject to complex disturbances and measurement noises," IEEE/CAA Journal of Automatica Sinica, vol. 8, no.9, pp1576-1587, 2021.

[3] S. Gao, and J. Liu, "Adaptive neural network vibration control of a flexible aircraft wing system with input signal quantization," Aerospace Science and Technology, vol. 96, pp105593, 2020.

[4] Q. Hu, "Sliding mode maneuvering control and active vibration damping of three-axis stabilized flexible spacecraft with actuator dynamics," Nonlinear Dynamics, vol. 52, no.3, pp227-248, 2008.

[5] B. Xiao, Q. Hu, and Y. Zhang, "Adaptive sliding mode fault tolerant attitude tracking control for flexible spacecraft under actuator saturation," IEEE Transactions on Control Systems Technology, vol. 20, no.6, pp1605-1612, 2011.

[6] C. Zhong, Z. Chen, and Y. Guo, "Attitude control for flexible spacecraft with disturbance rejection," IEEE Transactions on Aerospace and Electronic Systems, vol. 53, no.1, pp101-110, 2017.

[7] C. Dong, L. Xu, Y. Chen, and Q. Wang, "Networked flexible spacecraft attitude maneuver based on adaptive fuzzy sliding mode control," Acta Astronautica, vol. 65, no.11-12, pp1561-1570, 2009.

[8] J. Zhong, S. Liang, Q. Xiong, M. Gao, and K. Wang, "Receding horizon guaranteed cost control for norm-bounded uncertain systems with actuator saturation," Proceedings of 2017 IEEE Conference on Control Technology and Applications (CCTA) 2017, IEEE, pp1746-1750.

[9] W. Qi, X. Gao, and Y. Li, "Robust H-infinity control for stochastic Markovian switching systems under partly known transition probabilities and actuator saturation via anti-windup design," Circuits, Systems, and Signal Processing, vol. 34, no.7, pp2141-2165, 2015.

[10] W. Liu, Y. Wei, and G. Duan, "Barrier Lyapunov function-based integrated guidance and control with input saturation and state constraints," Aerospace Science and Technology, vol. 84, pp845-855, 2019.

[11] L. Lao, M. Ellis, and P. D. Christofides, "Handling state constraints and economics in feedback control of transport-reaction processes," J. Process Control, vol. 32, pp98-108, 2015.

[12] T. Hu, Z. Lin, and B. M. Chen, "An analysis and design method for linear systems subject to actuator saturation and disturbance," Automatica, vol. 38, no.2, pp351-359, 2002.

[13] L. Sun, "Disturbance observer-based saturated attitude tracking control of flexible spacecraft with measurement uncertainties," Proceedings of 2019 Chinese Control Conference (CCC) 2019, IEEE, pp358-363.

[14] D. Panagou, D. M. Stipanović, and P. G. Voulgaris, "Distributed coordination control for multi-robot networks using Lyapunov-like barrier functions," IEEE Transactions on Automatic Control, vol. 61, no.3, pp617-632, 2015.

[15] M. TayyebTaher, and S. M. Esmaeilzadeh, "Model predictive control of attitude maneuver of a geostationary flexible satellite based on genetic algorithm," Adv. Space Res., vol. 60, no.1, pp57-64, 2017.

[16] N. M. Horri, P. L. Palmer, and M. Roberts, "Energy optimal spacecraft attitude control subject to convergence rate constraints," Control Engineering Practice, vol. 19, no.11, pp1297-1314, 2011.

[17] F. Wang, Q. Zong, and B. Tian, "Adaptive backstepping finite time attitude control of reentry RLV with input constraint," Mathematical Problems in Engineering, vol. 2014, 2014. https://doi.org/10.1155/2014/801747

[18] A. M. Zou, K. D. Kumar, and A. H. de Ruiter, "Robust attitude tracking control of spacecraft under control input magnitude and rate saturations," International Journal of Robust and Nonlinear Control, vol. 26, no.4, pp799-815, 2016.

[19] Z. Liu, J. Liu, and L. Wang, "Disturbance observer based attitude control for flexible spacecraft with input magnitude and rate constraints," Aerospace Science and Technology, vol. 72, pp486-492, 2018.

[20] S. M. Rad, A. Khosravi, and P. Sarhadi, "Pitch autopilot design for an autonomous aerial vehicle in the presence of amplitude and rate saturation," Aerospace Science and Technology, vol. 108, pp106371, 2021.

[21] S. Wu, W. Chu, X. Ma, G. Radice, and Z. Wu, "Multi-objective integrated robust H∞ control for attitude tracking of a flexible spacecraft," Acta Astronautica, vol. 151, pp80-87, 2018.

[22] S. Wu, and S. Wen, "Robust H∞ output feedback control for attitude stabilization of a flexible spacecraft," Nonlinear Dynamics, vol. 84, no.1, pp405-412, 2016.